JAST, Vol. 2, No. 4, pp 55–63

JAST
Journal of Aerospace Science and Technology

Orr Sommerfeld Solver Using Mapped Finite Difference Scheme for Plane Wake Flow

M. J. Maghrebi[1]

Linear stability analysis of the three dimensional plane wake flow is performed using a mapped finite difference scheme in a domain which is doubly infinite in the cross–stream direction of wake flow. The physical domain in cross–stream direction is mapped to the computational domain using a cotangent mapping of the form $y = -\beta cot(\pi\zeta)$. The Squire transformation [2], proposed by Squire, is also used to relate the three–dimensional disturbances to the equivalent two–dimensional disturbances. The compact finite difference scheme of Lele [3] and the chain rule of differentiation are used to solve the Orr Sommerfeld equation. The results of linear stability analysis indicates that streamwise and the spanwise component of velocity eigenmodes are antisymmetric and the cross stream velocity eigenmode is symmetric. This is consistent with the DNS requirement of plane wake flow pertaining to solvability conditions [5].

INTRODUCTION

Linear stability theory determines the amplification, or decay, of small velocity disturbances superimposed on the mean velocity of a fluid flow. This provides a valid solution in the linear flow regime. Classical linear stability analysis predicts a solution to the linearized Navier Stokes equations for a fluid which satisfies the parallel flow assumptions (the mean components of velocity are zero except for the mean streamwise velocity which is assumed to be a y–dependent function). Therefore, it can be used as a verification tool to determine the accuracy of the numerical simulation, provided that the assumption of parallel flow is satisfied and very small amplitude forcing perturbations are used. Since the wake flow develops linearly at the early stages of its evolution (Sato & Kuriki [8], the inlet boundary conditions of the computational domain are specified using the solution of linear stability calculations. This is performed by solving the Orr–Sommerfeld equation which is an eigenvalue problem. In the what follows the governing equation of the eigenvalue problem is derived. The solution procedure is presented and the solutions are compared with reference to published results.

1. *Associate Professor, Dept. of Mechanical Eng., Shahrood Univ. of Tech., Shahrood, I.R.IRAN, Email: javad@shahrood.ac.ir.*

DERIVATION OF THREE–DIMENSIONAL LINEARIZED DISTURBANCE AND ORR–SOMMERFELD EQUATIONS

The theory of linear stability analysis is based on linearized equations of motion (Linearized form of the Navier Stokes equations). It is worth mentioning that the Navier Stokes equation is assumed to be normalized by appropriate length and velocity scales through the use of the next three assumptions.

1. Decomposing the pressure and velocity components into mean parts ($U(y)\underline{i}$ and $P(x,y,z)$) and fluctuating parts ($\underline{u'}(x,y,z,t)$ and $p'(x,y,z,t)$). In other words:

$$\underline{u}(x,y,z,t) = U(y)\underline{i} + \underline{u'}(x,y,z,t), \quad (1)$$

$$p(x,y,z,t) = P(x,y,z) + p'(x,y,z,t), \quad (2)$$

where $\underline{i}$ is the unit vector in the streamwise direction.

2. The perturbation components are assumed to be small such that all quadratic terms in the fluctuating components can be neglected with respect to the linear terms.
3. The mean parts are the solutions of the Navier Stokes equations.

the linearized equation of motion Eq. (3)

$$\frac{\partial \underline{u'}}{\partial t} + U(y)\frac{\partial \underline{u'}}{\partial x} + v'\frac{dU}{dy}\underline{i} = -\nabla p' + \frac{1}{Re}\nabla^2 \underline{u'}, \quad (3)$$

$$\nabla.\underline{u}' = 0. \tag{4}$$

can be derived by simplifying the Navier Stokes equations.

Note that a y dependent mean part is assumed for the streamwise velocity while zero value is taken for the mean component of velocity in the spanwise and cross–stream directions. In other words, the flow is assumed to be parallel. The fluctuating parts are assumed to be in the form of travelling wave:

$$\underline{u'}(x,y,z,t) = \underline{\hat{u}}(y).\exp(i(\alpha x + \beta z - \omega t)), \tag{5}$$

$$p'(\underline{x},t) = \hat{p}(y).\exp(i(\alpha x + \beta z - \omega t)). \tag{6}$$

β and the real part of α determine the wavelength in spanwise (z) and streamwise (x) directions, respectively. ω and the imaginary part of α are the circular frequency and the spatial linear growth rate of the perturbation, respectively. The relationship between ω, α and complex wave speed (c) is given by $c = \omega/\alpha$. The real part of c denotes the wave speed in the streamwise direction for a temporally evolving flow, while the ratio of ω/α_r represents the wave speed in the streamwise direction of a spatially evolving flow. It can be easily verified by defining the wave speed (v_{wave}) as the velocity of a wave which travels one streamwise wavelength over a time period that:

$$v_{wave} = \lambda_x/T = (2\pi/\alpha_r)/(2\pi/\omega) = \omega/\alpha_r. \tag{7}$$

The wave speed can be used as a good estimate for the convection velocity at the outlet boundary [6]. The physical meaning in Eqs. (5) and (6) is attached to their real parts and the use of complex notation is only for the sake of simplicity and convenience. Substituting Eqs. (5) and (6) into the linearized equation of motion, forms Eqs. (8) through (11) for the velocity and pressure eigenmodes ($\underline{\hat{u}}(y)$ and $\hat{p}(y)$), respectively.

$$i\alpha(U-c)\hat{u} + U'\hat{v} = -i\alpha\hat{p} + \frac{1}{Re}[\hat{u}'' - (\alpha^2+\beta^2)\hat{u}], \tag{8}$$

$$i\alpha(U-c)\hat{v} = -D\hat{p} + \frac{1}{Re}[\hat{v}'' - (\alpha^2+\beta^2)\hat{v}], \tag{9}$$

$$i\alpha(U-c)\hat{w} = -i\beta\hat{p} + \frac{1}{Re}[\hat{w}'' - (\alpha^2+\beta^2)\hat{w}], \tag{10}$$

$$i(\alpha\hat{u} + \beta\hat{w}) + D\hat{v} = 0. \tag{11}$$

D is the first derivative operator in the cross –stream (y) direction of the flow.

Squire transformations, which relate the three–dimensional disturbances to the equivalent two–dimensional disturbances by Eqs. (12, 13, 14) [2]:

$$\tilde{\alpha}^2 = \alpha^2 + \beta^2, \tag{12}$$

$$\tilde{\alpha}\tilde{u} = \alpha\hat{u} + \beta\hat{w}, \tag{13}$$

$$\tilde{p} = (\tilde{\alpha}/\alpha)\hat{p}, \tag{14}$$

the spanwise component of the velocity eigenmode ($\hat{w}$) is eliminated from Eqs. (8) through (11). This forms:

$$i\tilde{\alpha}(U-\tilde{c})\tilde{u} + U'\tilde{v} = -i\tilde{\alpha}\tilde{p} + \frac{1}{\tilde{R}e}[\tilde{u}'' - \tilde{\alpha}^2\tilde{u}], \tag{15}$$

$$i\tilde{\alpha}(U-\tilde{c})\tilde{v} = -D\tilde{p} + \frac{1}{\tilde{R}e}[\tilde{v}'' - \tilde{\alpha}^2\tilde{v}], \tag{16}$$

$$i\tilde{\alpha}\tilde{u} + D\tilde{v} = 0. \tag{17}$$

Where

$$\tilde{v} = \hat{v}, \quad \tilde{c} = \hat{c}, \quad \tilde{R}e = Re(\frac{\alpha}{\tilde{\alpha}}).$$

By introducing a streamfunction as indicated by Eq. (18)

$$\psi(x,y,t) = \varphi(y)\exp(i\tilde{\alpha}(x-\tilde{c}t)), \tag{18}$$

which is related to the two–dimensional velocity components by Eqs. (19) and (20)

$$u(x,y,t) = \tilde{u}(y)\exp(i\tilde{\alpha}(x-\tilde{c}t)) = \frac{\partial\psi}{\partial y}, \tag{19}$$

$$v(x,y,t) = \tilde{v}(y)\exp(i\tilde{\alpha}(x-\tilde{c}t)) = -\frac{\partial\psi}{\partial x}, \tag{20}$$

relationships between the eigenfunction (φ) and the velocity and pressure eigenmodes are:

$$\tilde{u} = \frac{\partial\varphi}{\partial y}, \tag{21}$$

$$\tilde{v} = -i\tilde{\alpha}\varphi, \tag{22}$$

$$\tilde{p} = U'\varphi - (U-\tilde{c})\varphi' - \frac{1}{\tilde{\alpha}\tilde{R}e}(\varphi''' - \tilde{\alpha}^2\varphi'). \tag{23}$$

The choice of streamfunction is not arbitrary. It must exactly satisfy the continuity equation and be introduced in the form of a travelling wave. Now, the eigenvalue problem, known as the Orr–Sommerfeld equation, can be easily derived by substituting the velocity and pressure eigenfunctions Eqs. (22) and (23) in Eq. (16).

$$(U-\tilde{c})(\varphi'' - \tilde{\alpha}^2\varphi) - U''\varphi = \frac{-i}{\alpha Re}[\varphi'''' - 2\tilde{\alpha}^2\varphi'' + \tilde{\alpha}^4\varphi] \tag{24}$$

Note that $\alpha Re = \tilde{\alpha}\tilde{R}e$. A prime denotes the $D = \frac{d}{dy}$ operator. Since the Orr–Sommerfeld equation is a fourth order differential equation, it needs four boundary conditions. They are specified according to the conditions at the free–stream boundaries which suggest no perturbation (25) and no perturbation gradients at ($\pm\infty$). Hence, Dirichlet boundary conditions

Eq. (25) and Neumann boundary conditions Eq. (26) are specified for the Orr–Sommerfeld equation.

$$\varphi(+\infty) = \varphi(-\infty) = 0. \tag{25}$$

$$\varphi'(+\infty) = \varphi'(-\infty) = 0. \tag{26}$$

The matrix representation of the discretized Orr–Sommerfeld equation clearly shows the eigenvalue problem, that is:

$$A\varphi = \tilde{c}\varphi \tag{27}$$

where

$$A = (D^2 - \tilde{\alpha}^2 I)^{-1}[\Lambda_U(D^2 - \tilde{\alpha}^2 I) - \Lambda_{U''} + \frac{i}{\alpha Re}(D^2 - \tilde{\alpha}^2 I)] \tag{28}$$

I is an identity matrix of order N. N is the number of grid points used for discretization of the cross–stream direction. Λ_U and $\Lambda_{U''}$ are diagonal matrices containing the values of U and U'' at discrete y coordinates on the diagonal, respectively.

The spatial wavenumbers have to be specified for solving the eigenvalue problem. In other words, Eq. (27) offers a temporal eigenvalue problem rather than the spatial one. For solving the spatial Orr–Sommerfeld equation we cast it into a general temporal form with complex wavenumbers.

SOLUTION OF THE EIGENVALUE PROBLEM

Prior to evaluation of the matrix A in Eq. (27), which is a requirement of solving the Orr–Sommerfeld equation, we need to specify an oblique angle which is related to the wave speed in spatial directions x and z.

$$\theta = \tan^{-1}(v_x/v_z) \tag{29}$$

v_x and v_z in Eq. (29) are wavespeeds in the streamwise and spanwise directions of the flow, respectively. The oblique angle is also related to the spatial wavenumbers as follow.

$$\theta = \tan^{-1}\left(\frac{\lambda_x/T}{\lambda_z/T}\right) = \tan^{-1}\left(\frac{2\pi/\alpha_r}{2\pi/\beta}\right) = \tan^{-1}(\beta/\alpha_r)$$

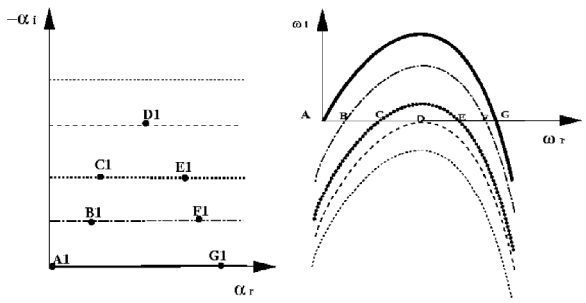

Figure 1. Mapping between complex planes of α and ω.

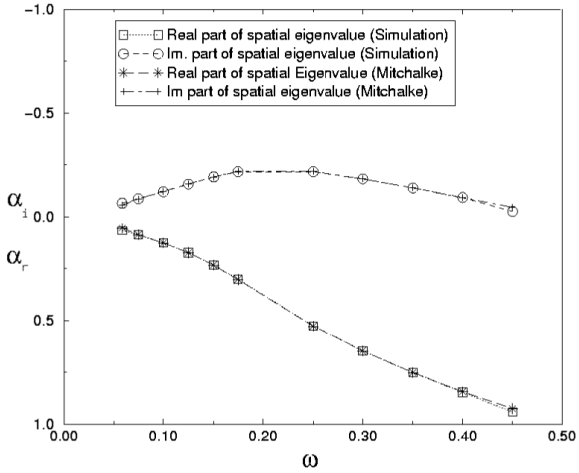

Figure 2. Comparison between spatial solution of Orr-Sommerfeld equation and results of Michalke [7] for U(y) = 0.5 (1 + tanh (y)).

As indicated in the previous section, there is no direct solution for the spatial eigenvalue problem because the matrix A of Eq. (27) cannot be evaluated. However, a complex mapping approach can be used to find the spatial solution. It can be performed by solving the temporal Orr–Sommerfeld equation for different complex wavenumbers, and computing the circular frequency (ω) where $\omega = \alpha C$ and C contains N different eigenvalues. Among the eigenvalues, the most amplified one, which grows the fastest is chosen. It relates to the solution with maximum of ω_i. Therefore, we can establish a mapping between a region in the complex space of α [pairs of (α_r, α_i)] and a region in the complex space of ω [pairs of (ω_r, ω_i)]. A schematic presentation of the mapping between these two regions is illustrated in Figure 1.

Corresponding to each α there is a most amplified temporal solution of the Orr–Sommerfeld equation for ω where both α and ω are complex numbers. The spatial solutions of the Orr–Sommerfeld equation (eigenvalues) are the spatial wavenumbers corresponding to the frequencies (ω's) with zero imaginary parts. This mutual correspondence between different α's (A_1,B_1,C_1,D_1,E_1,F_1 and G_1) and ω's (A,B,C,D,E,F and G) are also shown in Figure 1. For a given combination of $U(y)$, Re and oblique angle relationships between each components of the spatial eigenvalues with the circular frequency ($\alpha_r = \mathcal{F}_1(\omega_r)$ and $\alpha_i = \mathcal{F}_2(\omega_r)$) can be established. The established relationships ($\mathcal{F}_1(\omega_r)$ and $\mathcal{F}_2(\omega_r)$) can be immediately used to specify the spatial eigenvalues and eigenvectors for any frequency. To generate the relationships curve fitting methods were used for the pairs of data [(ω_r, α_r) and (ω_r, α_i)]. The data is collected by changing the real and imaginary part of α in two successive loops. The inner and outer loops change the real part and imaginary part of α, respectively. The following

considerations are taken into account to specify the range of the loops.

1. To obtain a positive amplification rate, the imaginary part has to be negative which can be easily checked by examining Eq. (5). This indicates that the maximum value of α_i is zero. Corresponding to this line there is a curve in space of ω which crosses the line of $\omega_i = 0$. They are point A and G of Figure 1.
2. To obtain enough spatial solution distributed over whole range of ω_r, we need to adjust the minimum value and the increment of α_i. α_i smaller than the minimum value will never return any spatial solution. It corresponds to the lowest curve shown in Figure 1, which does not cross the axis of $\omega_i = 0$.
3. Minima of α_r corresponds to the maximum for the wavelength. Hence, the minimum value for α_r is zero.
4. To obtain two spatial solutions in space of ω by any line of α_i, the maximum range and increment for α_r are specified. Computations for α_r which are larger than those of the maximum are not useful. This is because the curves will not cross the axis of $\omega_i = 0$ any more. Therefore, the three–dimensional spatial eigenvalue problem is solved according to the following steps.
   - $MIN(\alpha_i) \leq \alpha_i \leq 0$
     - $0 \leq \alpha_r \leq MAX(\alpha_r)$
       * calculate $\beta = \alpha_r \tan(\theta)$
       * calculate $\tilde{\alpha}^2 = \alpha^2 + \beta^2$
       * compute A of Eq. (27)
       * solve the eigenvalue problem
       * take the most amplified eigenvalue (corresponds to the one whose ω_i is smallest)
       * compute and store the spatial solutions (it happens, if there is a sign change between the current ω_i and that of the preceding)
   - Fit a function to the collected pairs which are smoothly distributed over the entire range of ω (e.g. $0 \leq \omega \leq \omega_{max}$), and check to ensure that the function well represents the data set. Note that any smooth curve fitting which represents the pair of data can be used. We use polynomials of order ten, which give a very smooth approximation to the pair of values.

Therefore, upon specifying $U(y)$, Re, θ and frequency, one can compute spatial wavenumbers simply by a function evaluation. Computation of eigenvectors corresponding to the spatial eigenvalue is easily determined. The solution to the two–dimensional equivalent of the three–dimensional Orr–Sommerfeld equation is now complete. The solution of eigenvalue problem is

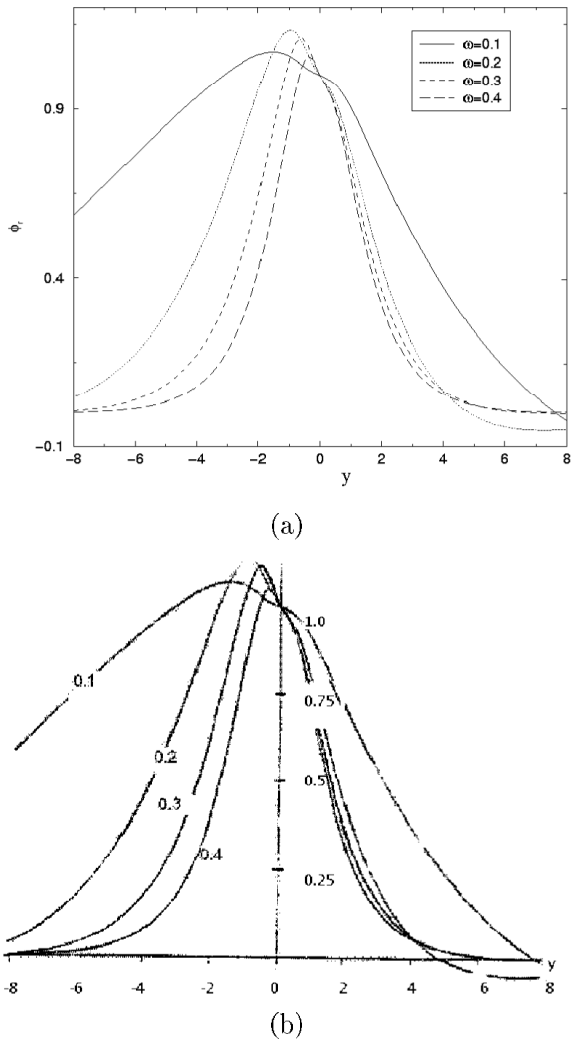

Figure 3. Comparison between real part of 2D Rayleigh eigenfunction solution and results of Michalke [7] for U(y) = 0.5 (1 + tanh (y)): (a) solution from Orr-Sommerfeld equation, (b) Michalke's results.

followed by determining the three–dimensional velocity eigenvectors which are used to generate perturbations for the numerical simulation of spatially–developing wake flow.

SOLUTION OF THE VELOCITY EIGENVECTORS

The three–dimensional linearized Navier Stokes Equation has been reduced to an equivalent two–dimensional eigenvalue problem (known as Orr–Sommerfeld equation) by the use of parallel flow assumption, travelling wave representation for the fluctuating parts of the pressure, velocity components (Eqs. (5) and (6)) and Squire's transformation (Eqs. (12), (13) and (14)). The eigenvector calculation in the previous section corresponds to the two–dimensional equivalents of the three–dimensional disturbances. Velocity and pressure eigenvectors of the equivalent two–dimensional distur-

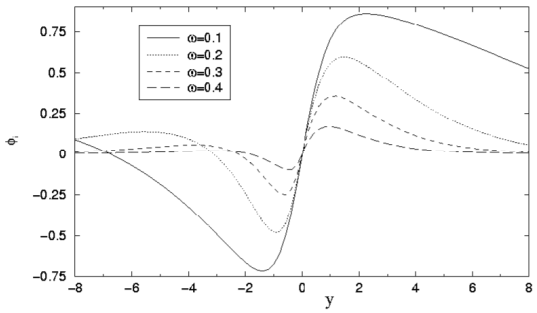

(a)

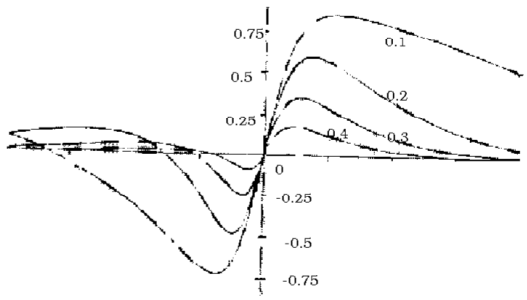

(b)

Figure 4. Comparison between imaginary part of 2D Rayleigh eigenfunction solution and results of Michalke [7] for U(y) = 0.5 (1 + tanh (y)), (a) solution from DNS, (b) Michalke's results.

bances can be directly determined by evaluating the right–hand side of Eqs. (21), (22) and (23) respectively. The three–dimensional disturbances can be recovered upon using $\hat{c} = \tilde{c}$, $\hat{w} = \tilde{w}$, $\hat{p} = \tilde{p}\frac{\alpha}{\tilde{\alpha}}$ and solving Eqs. (8) and (10). Extracting $\hat{u}$ and $\hat{w}$ from Eqs. (8) and (10) requires the solution of a complex matrix equation which is easily implemented. Linear stability calculations have been performed in the physical space of y with stretched grid discretization, using the compact finite difference scheme of Lele [3].

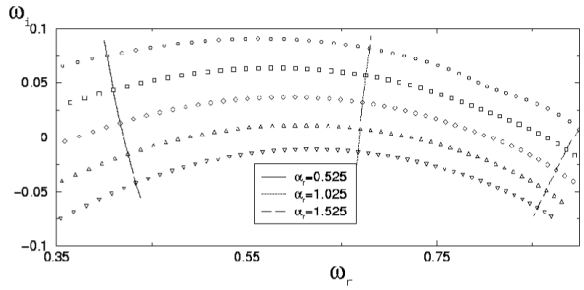

Figure 5. Orthogonality relationship between lines of α_r and α_i in space of ω (Five parallel curves, from top to the bottom, correspond to α_i = - 0.026, α_i = - 0.078, α_i = - 0.13, α_i = - 0.18 and α_i = - 0.234).

DERIVATIVE OPERATOR IN THE CROSS–STREAM DIRECTION USING COMPACT FINITE DIFFERENCE SCHEMES

In order to solve the Orr–Sommerfeld equation the second derivative operator in the cross–stream direction needs to be specified. A cotangent mapping given by:

$$y = -\beta \cot(\pi\zeta) \tag{30}$$

is used to map the doubly infinite domain ($-\infty \leq y \leq \infty$) into a unit interval domain ($0 \leq \zeta \leq 1$). β in Eq. (30) is the mapping parameter. The grid spacing in the unit interval are equally spaced. Thus, we can directly apply the compact finite difference scheme of Lele [3] to compute the derivative in the unit interval domain. However, we must use the chain rule of differentiation to find the derivative or the derivative operator in the physical domain of y. Application of the chain rule for the first and second derivatives results in Eqs. (31) and (32).

$$\frac{df}{dy} = \frac{df}{d\zeta}\frac{d\zeta}{dy} = \frac{\sin^2(\pi\zeta)}{\pi\beta}\frac{df}{d\zeta} \tag{31}$$

$$\frac{d^2f}{dy^2} = (\frac{\sin^2(\pi\zeta)}{\pi\beta})^2\frac{d^2f}{d\zeta^2} + \frac{2\sin^3(\pi\zeta)\cos(\pi\zeta)}{\pi\beta^2}\frac{df}{d\zeta} \tag{32}$$

Padé finite difference schemes, which is also used for approximation of derivatives in the streamwise direction in the full DNS code [5] are employed here to compute the derivatives in the unit interval domain. e.g.

$$f'_{j-1} + \frac{1}{\alpha}f'_j + f'_{j+1} = \frac{1+\frac{2}{\alpha}}{3\Delta x}(f_{j+1} - f_{j-1}) + \frac{4-\frac{1}{\alpha}}{12\Delta x}(f_{j+2} - f_{j-2}) \tag{33}$$

and

$$f''_{j-1} + \frac{1}{\alpha}f''_j + f''_{j+1} = \frac{4(\frac{1}{\alpha}-1)}{3\Delta x^2}(f_{j-1} - 2f_j + f_{j+1}) + \frac{10-\frac{1}{\alpha}}{12\Delta x^2}(f_{j-2} - 2f_j + f_{j-2}) \tag{34}$$

for the first and second derivative approximations. For the sake of brevity, the Padé finite difference scheme for the first and second derivative are written in the matrix form:

$$A_1\frac{df}{d\zeta} = B_1 f \tag{35}$$

and

$$A_2\frac{d^2f}{d\zeta^2} = B_2 f \tag{36}$$

where, the elements of matrix A_1, B_1, A_2 and B_2 are given by Eqs. (34) and (35), respectively. It is now straight forward to derive the first and second derivative operators in the cross–stream direction. They are given in the matrix form by Eqs. (37) and (38), respectively.

$$D = \Lambda_1 A_1^{-1} B_1 \tag{37}$$

$$D^2 = \Lambda_2 A_2^{-1} B_2 + \Lambda_3 A_1^{-1} B_1 \tag{38}$$

where, Λ_1,Λ_2 and Λ_3 are diagonal matrices with values of $\frac{\sin^2(\pi\zeta)}{\pi\beta}$, $(\frac{1}{\pi\beta}\sin^2(\pi\zeta))^2$ and $\frac{2}{\pi\beta^2}\sin^3(\pi\zeta)\cos(\pi\zeta)$ on the diagonal. Note that the boundary conditions are satisfied by default because the first and last terms of the diagonal matrices (Λ_1,Λ_2 and Λ_3) are zero. The second derivative operator (Eq. (38)) is used for evaluating the matrix A in (Eq. (27)) which is required for solving the Orr–Sommerfeld equation. The third derivative approximation (in Eq. (23)) is determined upon successive application of Eqs. (31) and (32).

COMPARISON BETWEEN THE SOLUTIONS OF THE ORR–SOMMERFELD EQUATION AND PREVIOUSLY PUBLISHED RESULTS

The results of Orr–Sommerfeld equation solution have been compared with the two–dimensional spatially–developing inviscid shear layer calculation of Michalke [7]. He used a numerical integration approach to solve the Rayleigh (inviscid Orr–Sommerfeld) equation. The comparison of the present results with Michalke's result is shown in Figure 2 which indicates excellent agreement.

The results of the most amplified eigenvector have also been compared with the results in [7], where the complex normalization factor, $(1/[\varphi_r(0) + i\varphi_i(0)])$ has been taken into account. Figure 3 and Figure 4 show the real and imaginary part of the eigenfunctions of the Rayleigh equation for the shear layer profile of $U(y) = 0.5(1 + \tanh(y))$ at different frequencies. Excellent agreement can be observed between the solutions obtained here and the results of Michalke [7].

The accuracy of the numerical technique, used for solving the Orr–Sommerfeld equation, can also be checked by investigating the relationship between the lines of α_r and α_i in the coordinate system of (ω_r, ω_i). They are expected to be orthogonal except at some singular points [1]. The orthogonality relationship is clearly indicated by Figure 5 for a wake flow with the mean velocity profile of $U(y) = 1 - 0.692\exp(-0.69315y^2)$ and $Re = 500$. The five curves in Figure 5 from top to the bottom, which are almost parallel, correspond to $\alpha_i = -0.026$, $\alpha_i = -0.078$, $\alpha_i = -0.13$, $\alpha_i = -0.18$ and $\alpha_i = -0.234$.

The effects of Reynolds number on the most unstable spatial wavenumber are shown in Figure 6. It indicates that the maximum spatial growth rate corresponds to the inviscid wake flow and that the effect of Reynolds number is not significant in determining the most unstable spatial wavenumber.

Figure 7 shows the spatial growth rate and the wavelength for a two–dimensional and three–dimensional mean wake profiles of $U(y) = 1 - 0.692\exp(-0.69315y^2)$ at $Re = 500$ and $\theta = 60°$. The figure indicates that the frequency corresponding to the maximum growth rate of three–dimensional disturbance is half of the two–dimensional one.

Figure 8 shows the eigenvectors for the most unstable solution for the two–dimensional and three–dimensional eigenvalue problems. These results show that the solutions are symmetric which offers an antisymmetric profile for the streamwise velocity eigen-

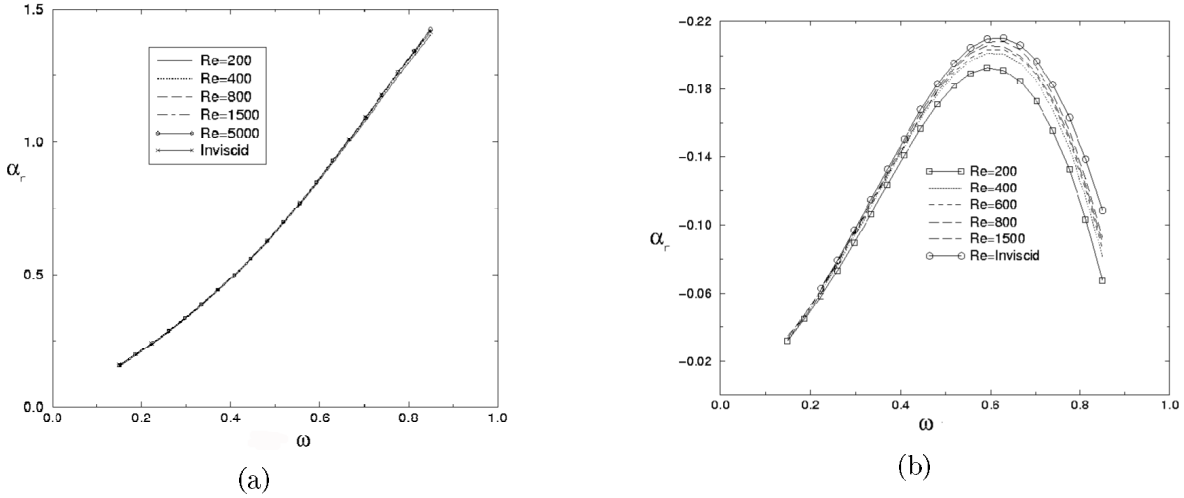

(a) (b)

Figure 6. Effect of Reynolds number on α_r in (a) and α_i in (b) (by solving the 2D Orr-Sommerfeld equation for U(y) = 1-0.692 exp(-0.69315 y^2)).

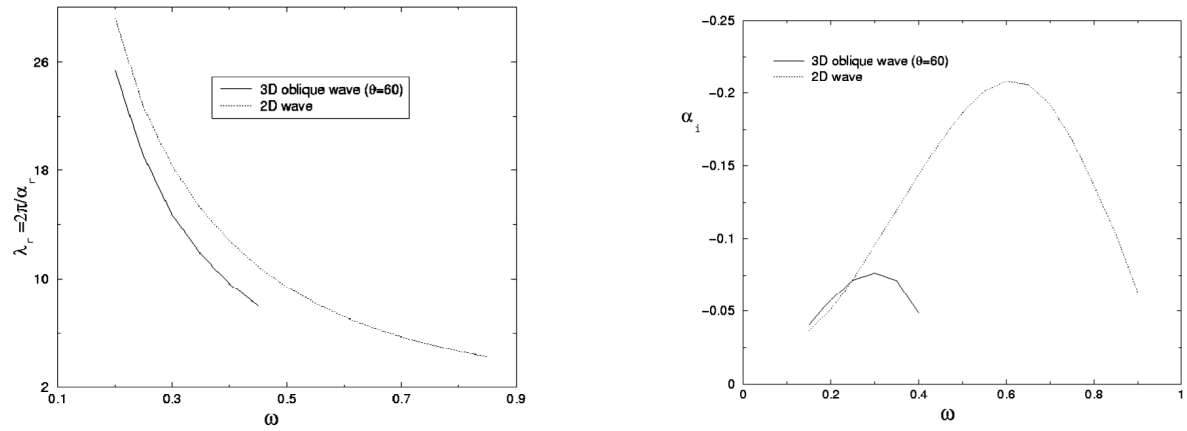

(a) (b)

Figure 7. 2D and 3D streamwise wavelength in (a) and growth rate in (b) (By solving Orr-Sommerfeld equation using U(y) = 1-0.692 exp(-0.69315 y^2), $Re = 500$ and θ=60°).

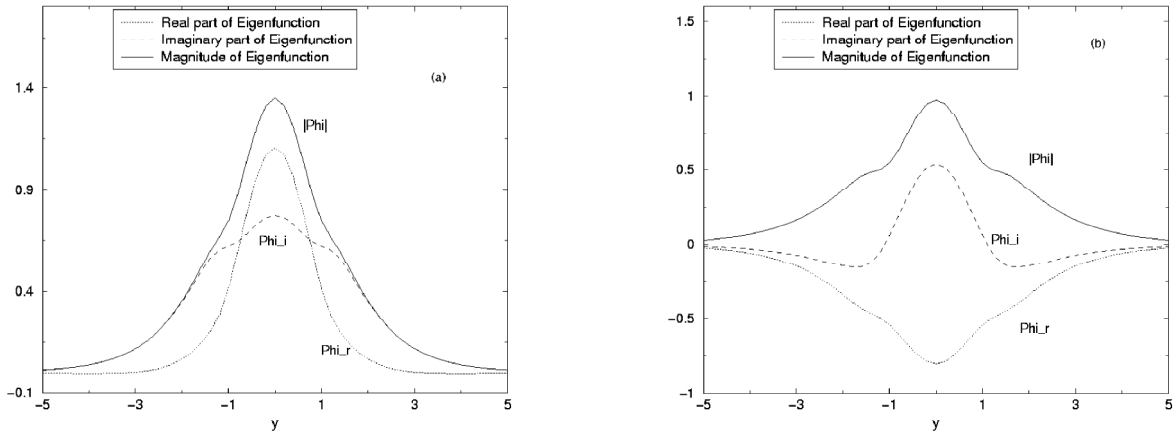

(a) (b)

Figure 8. Eigenfunctions corresponding to the most amplified eigenvalue of 2D (a) and 3D (b) Orr–Sommerfeld equation using U(y) =1-0.692 exp($-0.69315y^2$), $Re = 500$ and $\theta = 60°$

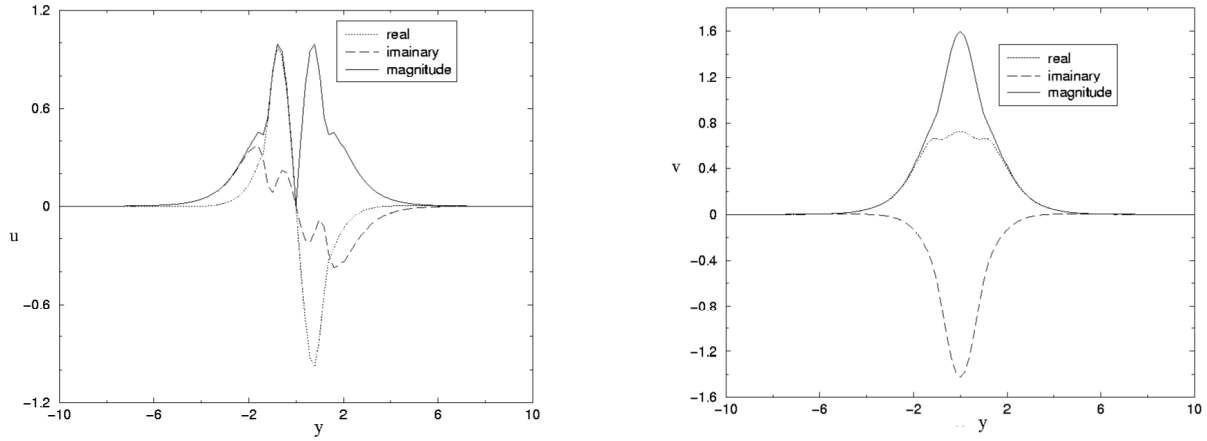

(a) (b)

Figure 9. 2D velocity eigenfunction components (By solving Orr-Sommerfeld equation using U(y) = 1-0.692 exp(-0.6931 y^2) and Re=500) for (a) streamwise, (b) cross–stream components.

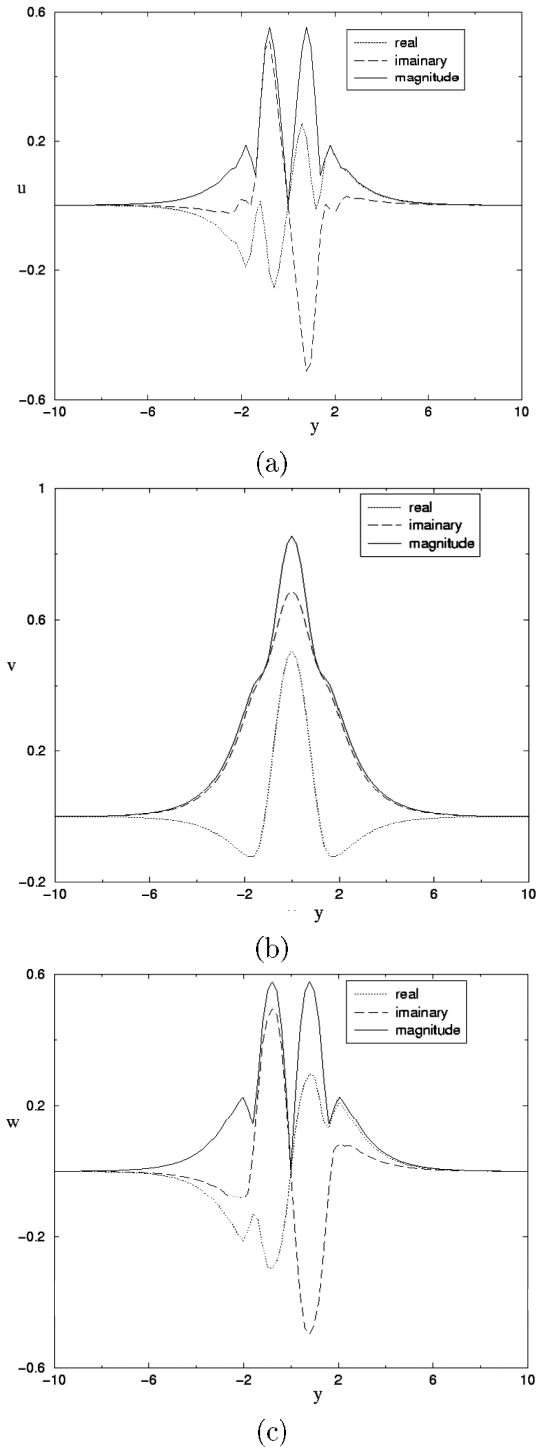

Figure 10. 3D velocity eigenfunction components (By solving Orr-Sommerfeld equation using U(y) = 1-0.692 exp(-0.6931y^2), Re=500 and θ=60°) for (a) streamwise, (b) cross-stream and (c) spanwise components.

vector (Figure 9(a)), and in the case of the three–dimensional problem, asymmetric profiles for streamwise and spanwise velocity eigenvectors (Figure 10 (a) and (c)). A requirement of the DNS simulation code refers to solvability condition by Maghrebi [5] which leads to selection of an antisymmetric profile for streamwise and spanwise velocity eigenvectors. These indicate that the eigenfunction of the Orr–Sommerfeld equation must be symmetric rather than antisymmetric. However, the use of an antisymmetric solution for a wake profile when the inflow boundary condition is perturbed by the cross–stream velocity component does not violate the solvability condition. This fact has been taken into account in the two–dimensional simulation of Maekawa *et al.* [4]. In fact, for any spatial simulation with random forcings at the inlet boundary, it is important to specify the cross–stream velocity as the inlet boundary condition. This is because the only requirement for the cross–stream velocity is to be zero at the free–stream boundaries ($\pm\infty$). Therefore, any kind of forcings obtained from the Orr–Sommerfeld equation can be used to specify the inlet boundary of the computational domain using the cross–stream velocity of the forcing. In other words v at the inflow boundary condition can be either symmetric, antisymmetric or any combinations of these two, while u and w at the inflow boundary must be presented by an antisymmetric profile in order to satisfy all of the solvability conditions. Figures 9 and 10 also indicate that all of the velocity eigenfunction profiles are zero at the free–stream boundaries and that the maximum variations of the velocity components occur at the wake center.

CONCLUSION

Linear stability analysis is performed to superimpose some perturbations on mean velocity profile at the inlet boundary of computational domain of full three–dimensional plane wake flow. The Physical domain of wake flow in cross–stream direction is mapped to a unit interval domain by the use of a cotangent mapping. The chain rule of differentiation and the compact finite difference scheme are used to generate the eigenvalue problem. Squire transformation and application of parallel flow assumption are employed to generate the eigenvalue problem obtained by linearizing the equation of motions for the full three–dimensional incompressible plane wake flow. Since The direct Orr–Sommerfeld equation offers a temporal eigenvalue problem, hence an indirect Orr–Sommerfeld equation is worked out for spatial eigenvalue problem. The numerical modeling of Orr–Sommerfeld equation is discussed and full verification is performed to make sure that the inflow boundary conditions of are set as we expect. The velocity eigenfunctions obtained from Orr–Sommerfeld equation indicates that they are consistent with DNS requirement of plane wake flow [5].

REFERENCES

1. Betchov R. and Criminale W. O., *Stability of Parallel Flow*, New York, Academic Press, (1967).
2. Drazin P. G., *Hydrodynamic Stability*, Cambridge University Press, (1981).
3. Lele, S. K., "Compact Finite Difference Schemes with Spectral–Like Resolution", *J. Comp. Phys.*, **103**, PP 16-42(1992).
4. Maekawa H. and Mansour N. N., "Direct Numerical Simulations of a Spatially–Developing Plane Wake", *JSME International Journal*, **35(**4), PP 543-548(1992).
5. Maghrebi M. J., "A Study of the Evolution of Intense Focal Structures in Spatially–Developing Three–Dimensional Plane Wakes", Ph.D. Thesis, Department of Mechanical Engineering, Monash University, Melbourne, Australia(1999).
6. Michalke A., "On Spatially Growing Disturbances in an Inviscid Shear Layer", *J. Fluid Mech*, **23**, PP 521-544(1965).
7. Sato H. and Kuriki K., "The Mechanism of Transition in the Wake of a Thin Flat Plate Placed Parallel to a Uniform Flow", *J. Fluid Mech*, **11**, PP 321-352(1961).